Atomic cascade in muonic hydrogen and the problem of kinetic-energy distribution in the ground state

V. E. Markushin*
Russian Research Center, Kurchatov Institute, Moscow 123182, Russia
(Received 24 January 1994)

The deexcitation of μp and μd atoms has been simulated within a kinetics model, taking the energy dependence of cascade processes into account. The x-ray yields and the kinetic-energy distributions for the ground and excited states have been calculated. The high-energy component produced by the Coulomb deexcitation is shown to result in noticeable effects in precise x-ray spectroscopy and muonic-atom diffusion.
PACS number(s): 36.10.Dr

I. INTRODUCTION

The muonic atoms of hydrogen isotopes, μp, μd, and μt, are the simplest among the exotic atoms, and have been studied for many years both experimentally [1–7] and theoretically [8–12].

The atomic cascade in the light muonic atoms is not influenced by strong interactions that occur in hadronic atoms such as $\pi^- p$ and $p\bar{p}$, and therefore it can be used as a "pure" probe of the deexcitation processes. The formation and deexcitation of muonic atoms are also important in various phenomena such as muonic-atom diffusion [13, 14], muon catalyzed fusion [15], muon transfer [12, 16, 17], and weak muon absorption; in considering these processes, one also needs rather detailed information about the muonic-atom kinetic-energy distribution.

Some basic features of the atomic cascade, including the density dependence of the x-ray yields and the cascade time, can be successfully described by the standard cascade model introduced in [18] and developed in [9, 10] (see [19, 20], and references therein). In this model it is assumed that the interplay between atomic internal and external degrees of freedom can be neglected, and the kinetic energy of the atom is treated as a fitting parameter used in the calculations of energy-dependent kinetics rates.

In order to investigate the atomic cascade beyond the standard cascade model, the Mainz cascade model was suggested and developed [21–24]. In this model the collisional processes were simulated by the classical-trajectory Monte Carlo method. Since this method allows one to account for the influence of the target atomic electric field on the exotic atom trajectory, the tuning parameters for the Stark mixing collisions can be removed. The Mainz model was successfully used to describe antiprotonic hydrogen [24], as well as exotic helium atoms [21, 22]. However, no significant dependence of the results on the kinetic energy was found in this model, and the problem of acceleration and deceleration has not been considered.

The problem of the time evolution of the kinetic-energy distribution during the cascade was discussed within a simplified cascade model in [25]. A significant fraction of the atoms was shown to stay in the so-called epithermal state, with characteristic kinetic energy about 1 eV due to the interaction of the dipole moment of the muonic atom with the external atomic electric field during the Auger transitions.

The conventional wisdom that the kinetic energy of an exotic hydrogen is of the order of eV [18] had to be revised following the measurements of the neutron time of flight for the charge exchange reaction $\pi^- p \to \pi^0 + n$ in liquid hydrogen [26], where a significant fraction of $\pi^- p$ atoms (about 50%) was found to be in a "hot" state at the instant of absorption, with mean kinetic energy of a few tens of eV's. The only known mechanism that can produce such a high-energy component is the Coulomb deexcitation [27]. The validity of the model used in [27] was questioned in the later investigations [25, 28], and no detailed calculations of Coulomb deexcitation effects at the end of the cascade have been done until now. However, neglecting the Coulomb deexcitation leads to a drastic contradiction with the pionic hydrogen data [26]. Now with new evidence of the high-energy component from the measurement of the reaction $\pi^- p \to \pi^0 + n$ at Paul Scherrer Institute [29], the problem of the Coulomb deexcitation effects in muonic atoms appears to be of considerable importance.

In order to provide a detailed theoretical background for the current studies of the muonic cascade in exotic atoms with $Z = 1$, a cascade model has been developed which includes both acceleration and deceleration of the exotic atom during the cascade. This paper focuses on the muonic cascade in hydrogen and deuterium in the density range $N = (10^{-5}\text{–}1)N_0$ where $N_0 = 4.25 \times 10^{22}$ cm^{-3} is the liquid hydrogen density (LHD). Detailed results for the muon transfer in the excited states in mixtures of hydrogen isotopes will be published elsewhere.

The paper is arranged as follows: the cascade model is described in Sec. II; the results of the cascade calculations are given in Sec. III; Sec. IV contains the discussion and concluding remarks.

*Electronic address: markushi@pliv.kiae.su

Until otherwise stated, all density-dependent rates are given for liquid hydrogen density. The muonic Bohr radius is $a_\mu = \hbar^2/m_\mu e^2 = 256$ fm, and the Coulomb binding energies of the μp and μd ground states are $\epsilon_{\mu p} = 2.529$ keV and $\epsilon_{\mu d} = 2.663$ keV.

II. CASCADE MODEL

A. Basic cascade processes

Our cascade model includes the deexcitation mechanisms accepted in the standard cascade model (see [9,10, 18–20], and references therein), with the muonic-atom energy being considered as a time-dependent distribution rather than a parameter; thus one of the main limitations of the standard cascade model has been removed.

The basic cascade processes and their main features are listed in Table I. The radiative deexcitation is the only cascade process which is energy and density independent. The n dependence of various cascade processes is shown in Fig. 1. Since the radiative deexcitation rates decrease rapidly with increasing n, only the collisional processes are important at the upper stage of the cascade. The lower the density, the more significant are the radiative transitions in the deexcitation process.

The Auger deexcitation rates calculated in the Born approximation [18] are energy independent. More refined consideration based on the eikonal approximation [11] results in rather weak energy dependence. Since both methods are in good agreement with each other at low n ($n \leq 6$), the former was used in the present calculations. Auger deexcitation is dominated by E1 transitions with the minimal change in principal quantum number n permitted for ionization of the hydrogen molecule. The Auger deexcitation rate reaches its maximum at $n = 7$ when the transitions $\Delta n = 1$ become possible, and with decreasing n the Auger rate falls rapidly as the size of the muonic atom becomes much smaller than the electron Bohr radius.

Stark mixing is the fastest collisional process, with the cross section scale being determined by the size of the hydrogen atom. Stark transitions were calculated in the straight line trajectory approximation [18] using the dynamical group method [30] by implicit integration over all impact parameters. The cross sections thus obtained are about 50% larger than those calculated in the effective impact parameter approximation [18, 9]. Stark mixing rates are monotonically increasing functions of energy and n, with the result of calculations being shown in Fig. 2. In order to account for uncertainties in the present model, one can use Stark mixing coefficient $k_{\rm Stk}$ (a factor multiplying all Stark mixing rates), which is known to be important, together with the effective kinetic energy, for fitting absorption fractions and x-ray yields in hadronic atoms [18, 29]. The results for muonic hydrogen, on the contrary, were found to be rather insensitive to variations of the Stark mixing coefficient in the range $k_{\rm Stk} = 1 - 2$ (unless the density is not very small: $N > 10^{-4} N_0$), since there is no absorption during the cascade in this case. For this reason, and also because the energy evolution is taken into account explicitly, the fixed value $k_{\rm Stk} = 1$ is used in the following calculations.

In the radiative and Auger processes the transition energy is carried away mainly by a light particle; therefore the recoil energy of the muonic atom is rather small ($E \ll 1$ eV). However, in Coulomb collisions the transi-

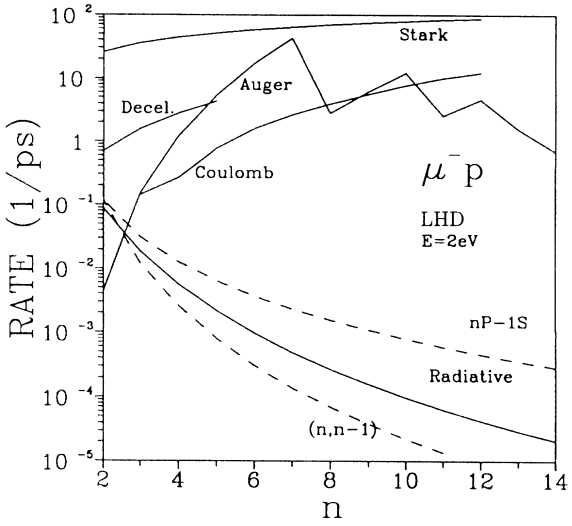

FIG. 1. The rates of various cascade processes vs initial state n for μp atom in liquid hydrogen. Statistical population of the nl sublevels is assumed. Also shown are the rates of the radiative transitions between the circular states $(n, n-1) \to (n-1, n-2)$ and for the K lines $(nP \to 1S)$.

TABLE I. Basic cascade processes and their energy and density dependence.

Process	Energy dependence	Density dependence	Refs.
Radiative $(\mu^- p)_i \to (\mu^- p)_f + \gamma$	no	no	
External Auger effect $(\mu^- p)_i + H_2 \to (\mu^- p)_f + e^- + {H_2}^+$	no (weak)	linear	[18, 11]
Stark mixing $(\mu^- p)_{nl} + H \to (\mu^- p)_{nl'} + H$	Fig. 2	linear	[18, 30]
Coulomb collisions $(\mu^- p)_i + p \to (\mu^- p)_f + p$, $n_f < n_i$	$\sim 1/\sqrt{E}$	linear	[27]
Elastic scattering $(\mu^- p)_n + H \to (\mu^- p)_n + H$	$\sim 1/\sqrt{E}$	linear	[31]

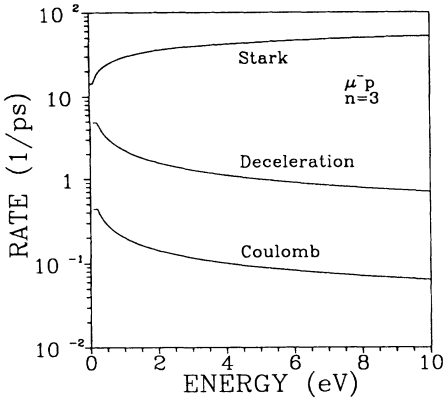

FIG. 2. The energy dependence of the Stark mixing, deceleration, and Coulomb deexcitation rates for μp atom in the state $n = 3$ in liquid hydrogen.

tion energy goes to the recoil of heavy particles, and $\mu^- p$ can gain about 30 eV as a result of transition $(n = 5) \rightarrow (n = 4)$ and 60 eV for $(n = 4) \rightarrow (n = 3)$. Those atoms with kinetic energy $E \gg 1$ eV form the so-called high-energy component of E distribution. Evidence for a large fraction of high-energy component ($\sim 50\%$) was found for $\pi^- p$ atoms at the instant of nuclear absorption ($n = 3, 4$) in liquid hydrogen [26]. Due to the similarity of the deexcitation of pionic and muonic atoms one can expect a significant high-energy component in muonic atoms as well.

Rates for the Coulomb deexcitation were calculated according to [27]. Using the rates thus calculated for the $\pi^- p$ atom, our cascade model predicts the high-energy component at the instant of nuclear absorption in liquid hydrogen to be about 50%, in good agreement with the experiment [26]. The rates shown in Fig. 1 were calculated at the atomic kinetic energy $E = 2$ eV.

Other possible acceleration mechanisms in atomic cascade include chemical deexcitation [18], and interaction of the atomic dipole moment with the external electric field during the Auger process [25]. Estimates show that these mechanisms can provide energy $E \sim 1$ eV to the muonic hydrogen atom. The characteristic energy of the atom at the instant of formation is also about 1 eV [35].

During the cascade the atom can lose its kinetic energy in elastic collisions. Using an estimate of deceleration rates [16], one finds that the initial energy distribution cannot remain unchanged until the final stage of the cascade because of multiple elastic scattering. However, the elastic scattering does not dominate the evolution of the energy distribution, and the atoms are not thermalized at the end of the cascade.

The first experimental evidence for a so-called epithermal energy distribution for light muonic atoms was found in muon catalyzed fusion [32,33] (see [15], and references therein). A direct probe of the energy distribution after the atomic cascade was provided by the observation of μd and μp diffusion in gas [13,14], and the characteristic kinetic energy of the muonic atoms in the ground state was measured to be $E \approx 1.2$ eV for μd and $E \approx 2$ eV for μp.

The deceleration due to elastic scattering was calculated in the classical motion approximation, using the exact terms for the Coulomb three-body problem [31]; the details will be published elsewhere. The deceleration rates shown in Fig. 1 were calculated with transport cross sections at $E = 2$ eV; energy-dependent differential cross sections were used in the cascade calculations.

Both Coulomb and deceleration cross sections calculated in the semiclassical approximation are inversely proportional to the collision energy. In order to regularize the low-energy behavior of these rates (Fig. 2), a constant-value cutoff below the c.m. collisional energy $T_{\rm cut} = 0.1$ eV was imposed.

B. Cascade kinetics calculations

The muon is captured into an atomic orbit with the size of the electron Bohr radius a_e, i.e., the cascade starts from a highly excited state with principal quantum number $n \approx (a_e/a_\mu) = (m_\mu/m_e)^{1/2} \approx 14$ [34]. The more elaborate capture model [35] that takes molecular effects into account predicts that the initial n distribution is peaked near $n = 12$.

In the density region $N = (10^{-4}\text{–}1)N_0$ we did not find the results to be very sensitive to small variations of initial n, or to the initial distribution over l sublevels for given state n, because in the beginning of the cascade the collisional transitions with $\Delta n \leq 3$ dominate the deexcitation, and the fast Stark mixing provides a statistical distribution over l.

Evolution of the kinetic-energy distribution was taken into consideration below $n = 6$. Above $n = 6$ only the collisional cascade processes are important under the experimental conditions specified; therefore the energy distribution developed at this stage does not depend on the density. As the cascade continues, the kinetics involves rather few energy-dependent rates, thus making it possible to avoid introducing multiple parameters for model tuning. Since the available information is not sufficient to study the details of the energy distribution at the intermediate stage of the cascade, Maxwellian distribution was assumed at $n = 6$, with the mean kinetic energy $\bar{E}_{n=6} = 2$ eV for μp and $\bar{E}_{n=6} = 1.2$ eV for μd being taken according to the measurements [13, 14].

The cascade calculations were made with a Monte Carlo code similar to that recently developed for the simulation of the kinetics of the muon catalyzed fusion [36]. For a given set of kinetics parameters, from 10^5 to 10^6 chains of the events were usually generated, the accuracy of the results for the x-ray yields being sufficient for comparison with the expected experimental data.

III. RESULTS OF CALCULATIONS

A. The x-ray yields

Figure 3 shows the results of the cascade calculations for the K x-ray yields. Radiative deexcitation dominates the population of the ground state in the entire density range, the total x-ray yield of K lines being $Y_{\rm tot}(K) = 1.00$ in gas at 1 atm and $Y_{\rm tot}(K) = 0.95$

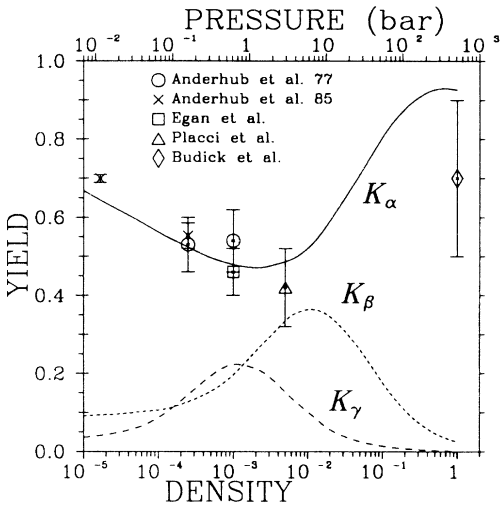

FIG. 3. The absolute K x-ray yields of muonic hydrogen vs density compared with the experimental data. The density is in units of the density of liquid hydrogen.

in liquid hydrogen. The calculated $K\alpha$ line yield is in good agreement with the experimental data [1–6] in the density region considered.[1]

As the density decreases, the radiative deexcitation stage starts earlier in the cascade. This can be seen in the $K\alpha$ yield, which goes down by a factor of 2 when liquid hydrogen is replaced by gas at 1 atm. The $K\beta$ yield reaches its maximum at about 10 atm, and the $K\gamma$ yield is maximal at about 1 atm.

There are experimental data available [5] at very low density where the x-ray yields are sensitive to the details of the atomic cascade at the high-n states. Detailed discussion of the features of the atomic cascade at low density will be published elsewhere.

B. The energy distribution

The calculated energy distributions at the end of the cascade are shown in Fig. 4 at various densities (47 mbar, 1 bar, 15 bars, and LHD). At very low density ($N \sim 10^{-5}N_0$) the energy distributions remain nearly unchanged at the lower stage of the cascade, and the ground state distribution is very close to that at $n = 6$. With increasing density the ground state energy distribution changes in two ways. First, some fraction of the low-energy component becomes less energetic due to multiple elastic collisions which result in the buildup of the thermal component at high density. Second, a high-energy component develops due to the Coulomb deexcitation, and its fraction grows with increasing density, as it is shown in Fig. 5.

[1]The data plotted in Fig. 3 have been renormalized using the total theoretical K x-ray yields.

IV. DISCUSSION

The theory predicts a strong density dependence of the x-ray yields in the density range $N = (10^{-3}–1)N_0$ (see Fig. 3) where few measurements with limited precision are available. The density dependence arises from the competition between the radiative and the collisional deexcitation, and therefore the measurements of the total absolute and relative $K\alpha$ and $K\beta$ x-ray yields with an accuracy of a few percent would allow one to test the collisional rates used in the calculations.

The role of the Coulomb deexcitation in the atomic cascade has been under discussion for a long time [27, 25, 28]. While the experimental data for pionic hydrogen [26] show evidence for a significant contribution of the Coulomb transitions, the corresponding effects in muonic atoms had not been considered until now. Our calculations using the rates from [27] demonstrate that the high-energy component for muonic hydrogen at the instant of reaching the ground state can be as large as 40% at the density $N = 0.01N_0$ (pressure about 10 bars) and about 50% in liquid hydrogen.

The density dependence of the high-energy fraction for μd is very close to that for μp (see Fig. 5), because the difference in the deexcitation rates is small. In particular, the Coulomb deexcitation rates are proportional to the factor $(ME)^{-1/2}$, where M and E are the mass and kinetic energy of the atom, so that the μp and μd have nearly equal Coulomb deexcitation rates at $E_{\mu p} \approx 2E_{\mu d}$.

The high-energy component can be studied experimentally by various methods. One is the measurement of the muonic atom diffusion between arrays of foils, which was successfully realized in the experiment [13, 14]. The calculated effect of the high-energy component at 100 mbar in the time distribution of the μd arriving at the foils[2] is shown in Fig. 6. The high-energy component results in significant enhancement at small times, the effect being easily visible even though the high-energy component is only 10% of the total energy spectrum.

The measurements done till now are not very sensitive to the details of the energy distribution (in particular, due to the limited time resolution). However, the increase of the mean kinetic energy with the density in the region from 47 mbar to 750 mbar found in [14] is in qualitative agreement with the cascade calculations. More detailed investigation of the energy distribution may be feasible by improving the time resolution of the detecting system to the level of 10 ns. The most favorable experimental conditions are expected to be at a density of about 100 mbar at the gap 1–2 mm, in this case the contribution of the high-energy component to the time distribution is not spread out much due to rescattering (the mean free

[2]The μd atoms are more suitable for studying this problem than the μp atoms due to the less important hyperfine structure effects and the smooth energy dependence of the scattering amplitude, see [14].

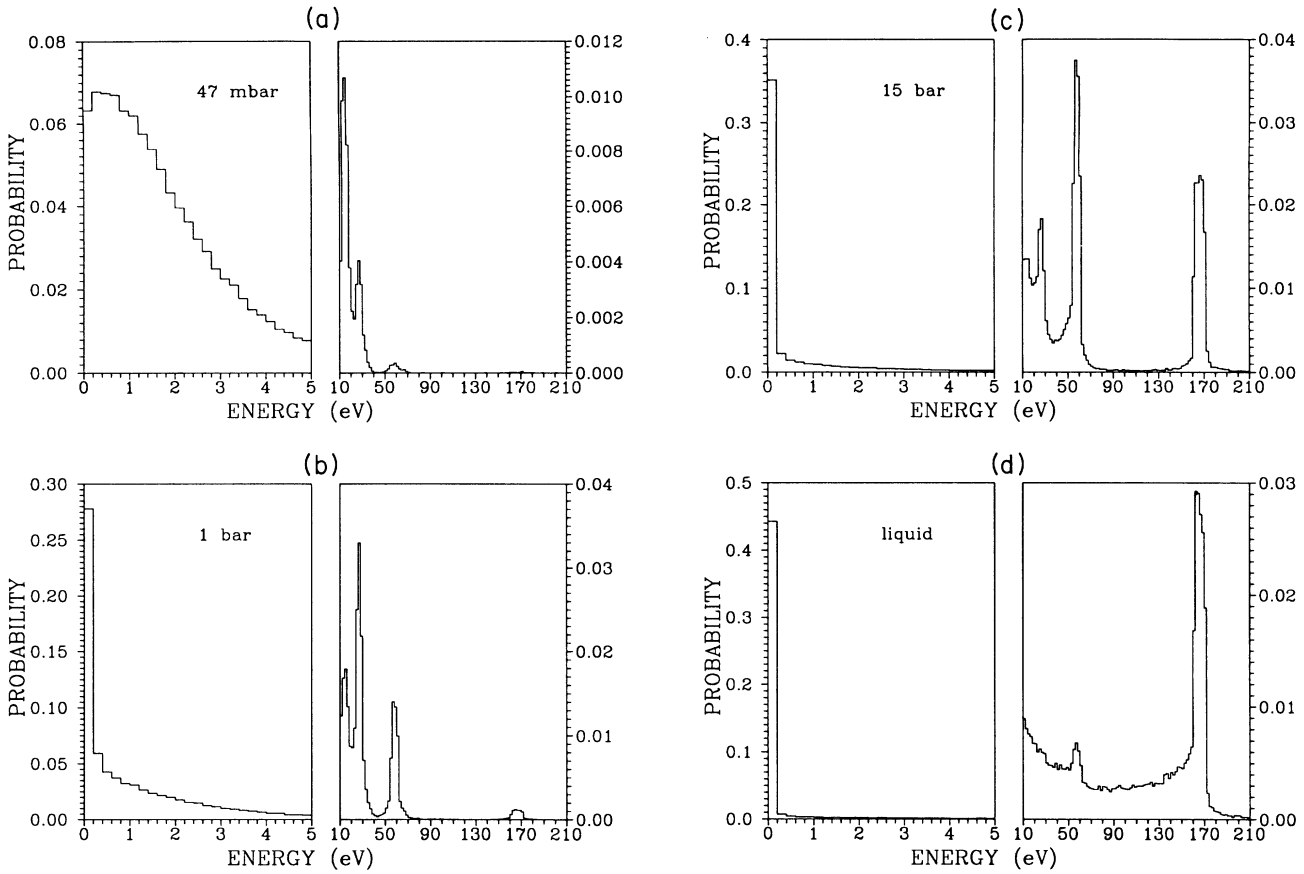

FIG. 4. The energy distribution of the μp atom at the end of the cascade: (a) gas at 47 mbar, (b) 1 bar, (c) 15 bars, (d) liquid hydrogen.

path and the gap are of the same order of magnitude).

Another method to investigate the energy distribution is based on the measurement of the Doppler broadening of the x-ray lines. This effect was discussed for pionic hydrogen in connection with precise measurements of the strong interaction effects (see [29], and references therein). In the case of muonic hydrogen and deuterium, the width of the line is not affected by nuclear interaction, so that μp and μd provide a good opportunity for direct study of the energy distribution in the *excited* states [37]. Figure 7 shows the energy distribution of the μp at the instant of the radiative deexcitation from the state $3P$ at 15 bars, in which case the total fraction of the high-energy component amounts to 50%. The x-ray line has a multicomponent profile with a characteristic central peak and high-energy pedestal, the latter having a significant spreading up to ± 0.8 eV for the $K\beta$ line.

This prediction can be tested by measurements of the Doppler broadening of the x-ray lines, using a high resolution crystal spectrometer system similar to that used for the determination of the strong interaction shift in pionic hydrogen [38]. Such measurements with very good statistics may be feasible with a cyclotron trap target system (see [39], and references therein).

The high-energy component may also result in some effects in muon catalyzed fusion similar to those discussed in [32, 33, 36]. Consideration of this problem is, however, beyond the scope of this paper.

In conclusion, using the atomic cascade model with time-dependent energy distribution, we found that Coulomb deexcitation results in a significant high-energy component in kinetic-energy distribution in the end of

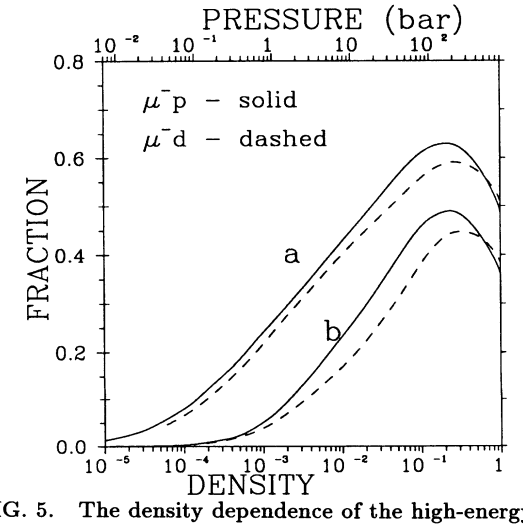

FIG. 5. The density dependence of the high-energy component fraction at the end of the cascade for the μp (solid line) and μd (dashed line) atoms: (a) $E > 8$ eV and (b) $E > 50$ eV. The density is in units of the density of liquid hydrogen.

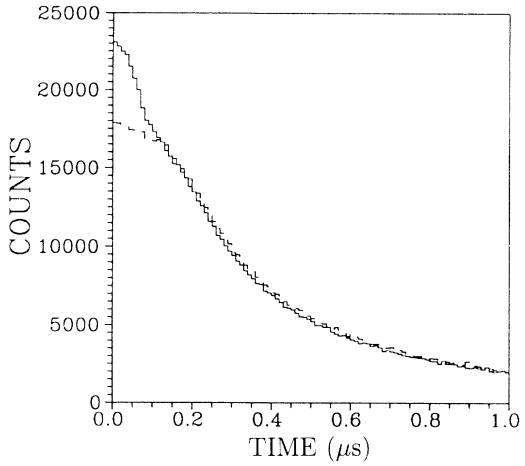

FIG. 6. The time distribution of the μd arriving at the array of foils with gap 2 mm at 100 mbar. The solid line is for the calculated energy distribution, the dashed line is for the same distribution with the high-energy component ($E >$ 8 eV) set to zero.

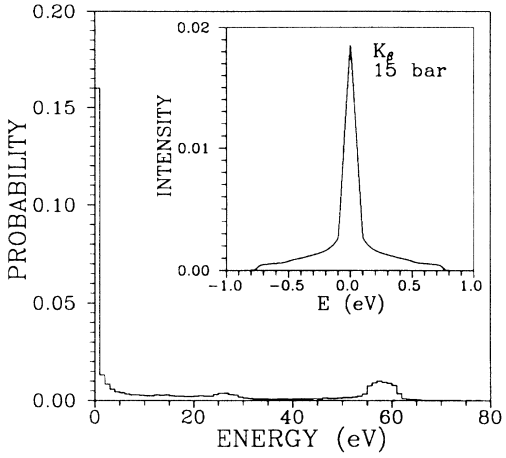

FIG. 7. The energy distribution of the μp atom at the instant of the radiative transitions $3P \rightarrow 1S$ at 15 bars and the $K\beta$ line profile (inset).

the cascade in the density range $(10^{-4}$–$1)N_0$. This result has been obtained with Coulomb deexcitation rates consistent with the measured high-energy component in pionic hydrogen [26]. Effects of the high-energy component can be observed in muonic hydrogen diffusion and the Doppler broadening of the x-ray lines, and the experimental investigations of these effects would be very valuable for the solution of the energy distribution problem. More refined calculations of the Coulomb transitions and the elastic collisions within the same framework at low n would also be desirable.

ACKNOWLEDGMENTS

The author wishes to thank Professor R. Siegel, Dr. L.M. Simons, and Dr. D.J. Abbott for numerous discussions, Dr. V.I. Savichev for his help in the calculation of the elastic cross sections, E.C. Aschenauer for assistance in developing the library of kinetics rates, and the Physics Department of the College of William and Mary, where part of this work was done, for kind hospitality. This work was supported in part by the U.S. National Science Foundation Grant No. NSF PHY-9115407.

[1] A. Placci, E. Polacco, E. Zavattini, K. Ziok, G. Carboni, U. Gastaldi, G. Gorini, and G. Torelli, Phys. Lett. **32B**, 413 (1970).

[2] B. Budick, J.R. Toraskar, and I. Yaghoobia, Phys. Lett. **34B**, 539 (1971).

[3] H. Anderhub, H. Hofer, F. Kottmann, P. LeCoultre, D. Makowiecki, O. Pitzurra, B. Sapp, P.G. Seiler, M. Walchli, D. Taqqu, P. Truttmann, A. Zehnder, and Ch. Tschalar, Phys. Lett. **71B**, 443 (1977).

[4] P.O. Egan, S. Dhawan, V.W. Hughes, D.C. Lu, F.G. Mariam, P.A. Souder, J. Vetter, G.zu Putlitz, P.A. Thompson, and A.B. Denison, Phys. Rev. A **23**, 1152 (1981).

[5] H. Anderhub, J. Bocklin, M. Devereux, F. Dittus, R. Ferreira Marques, H. Hofer, H.K. Hofer, F. Kottmann, O. Pitzurra, P.G. Seiler, D. Taqqu, J. Unternahrer, M. Walchli, and Ch. Tschalar, Phys. Lett. **101B**, 151 (1981).

[6] H. Anderhub, H.P. von Arb, J. Bocklin, F. Dittus, R. Ferreira Marques, H. Hofer, F. Kottmann, D. Taqqu, and J. Unternahrer, Phys. Lett. **143B**, 65 (1985).

[7] P. Ackerbauer, P. Baumann, E.D. Bovet, W.H. Breunlich, T. Case, D. Chattelard, K.M. Crowe, H. Daniel, J.-P. Egger, F.J. Hartmann, E. Jeannet, M. Jeitler, P. Kammel, B. Lauss, K. Lou, V. Markushin, J. Marton, C. Petitjean, W. Prymas, W. Schott, R.H. Sherman, T. von Egidy, P. Wojciechovski, and J. Zmeskal, PSI Proposal R-81-05, 1991, PSI Annual Report, 1992 (unpublished).

[8] M. Leon, Phys. Lett. **35B**, 413 (1971).

[9] E. Borie and M. Leon, Phys. Rev. A **21**, 1460 (1980).

[10] V.E. Markushin, Zh. Eksp. Teor. Fiz. **80**, 35 (1981) [Sov. Phys. JETP **53**, 16 (1981)].

[11] A.P. Bukhvostov and N.P. Popov, Zh. Eksp. Teor. Fiz. **82**, 23 (1982) [Sov. Phys. JETP **55**, 12 (1982)].

[12] W. Czaplinski, A. Gula, A. Kravtsov, A. Mikhailov, and N. Popov, Muon Catalyzed Fusion **5/6**, 55 (1990/91).

[13] J.B. Kraiman, G. Chen, P.P. Guss, R. Siegel, W. Vulcan, R. Welsh, W. Breunlich, M. Cargnelli, P. Kammel, J. Marton, J. Zmeskal, F. Hartmann, C. Petitjean, A. Zehnder, J. Reidy, and H. Woolverton, Phys. Rev. Lett. **63**, 1942 (1989).

[14] D.J. Abbott, J.B. Kraiman, R. Siegel, W. Vulcan, D.W. Viel, C. Petitjean, A. Zehnder, W. Breunlich, P. Kammel, J. Marton, J. Zmeskal, J. Reidy, H. Woolverton, and F. Hartmann, in *Muonic Atoms and Molecules*, edited by L.A. Schaller and C. Petitjean (Birkhäuser, Basel, 1993), p. 243.

[15] S.S. Gerstein, Yu.V. Petrov, and L.I. Ponomarev, Usp. Fiz. Nauk **160**, 3 (1990) [Sov. Phys. Usp. **33**, 591 (1990)]; C. Petitjean, Nucl. Phys. **A543**, 79 (1992).
[16] L.I. Menshikov and L.I. Ponomarev, Z. Phys. D **2**, 1 (1986).
[17] A.V. Kravtsov, A.I. Mikhailov, S.Yu. Ovchinnikov, and N.P. Popov, Muon Catalyzed Fusion **2**, 183 (1988).
[18] M. Leon and H.A. Bethe, Phys. Rev. **127**, 636 (1962).
[19] V.E. Markushin, in *EM Cascade and Chemistry of Exotic Atoms*, edited by L.M. Simons *et al.* (Plenum, New York, 1990), p. 73.
[20] F. Kottmann, in *Muonic Atoms and Molecules*, edited by L.A. Schaller and C. Petitjean (Birkhäuser, Basel, 1993), p. 219.
[21] R. Landua and E. Klempt, Phys. Rev. Lett. B **191**, 48 (1982).
[22] G. Reinfenröter, E. Klempt, and R. Landua, Phys. Lett. B **191**, 15 (1987).
[23] G. Reinfenröter, E. Klempt, and R. Landua, Phys. Lett. B **203**, 9 (1988).
[24] G. Reinfenröter and E. Klempt, Nucl. Phys. **A503**, 885 (1989).
[25] L.I. Menshikov, Muon Catalyzed Fusion **2**, 173 (1988).
[26] J.E. Crawford, M. Daum, R. Frosch, B. Jost, P.-R. Kettle, R.M. Marshall, B.K. Wright, and K.O.H. Ziock, Phys. Lett. B **213**, 391 (1988); Phys. Rev. D **43**, 46 (1991).
[27] L. Bracci and G. Fiorentini, Nuovo Cimento A **43**, 9 (1978).
[28] W. Czaplinski, A. Gula, A. Kravtsov, A. Mikhailov, N. Popov, and S. Ovchinnikov, Muon Catalyzed Fusion **5/6**, 59 (1990/91).
[29] E.C. Aschenauer, K. Gabathuler, J. Missimer, L.M. Simons, A. Badertscher, P.F.A. Goudsmit, H.J. Leisi, E. Matsions, H.C. Schröder, D. Sigg, Z.G. Zhao, D. Chatellard, J.-P. Egger, and V. Markushin (unpublished).
[30] J.-L.Vermeulen, Nucl. Phys. **B12**, 506 (1969).
[31] V.I. Savichev (unpublished).
[32] J.S. Cohen and M. Leon, Phys. Rev. Lett. **55**, 52 (1985).
[33] P. Kammel, Nuovo Cimento Lett. **43**, 349 (1985).
[34] J.S. Cohen, Phys. Rev. A **27**, 167 (1983).
[35] G.Ya. Korenman, V.P. Popov, and G.A. Fesenko, Muon Catalyzed Fusion **7**, 179 (1992).
[36] V.E. Markushin, E.I. Afanasieva, and C. Petitjean, Muon Catalyzed Fusion **7**, 155 (1992).
[37] L.M. Simons (private communication).
[38] W. Beer, M. Bogdan, P.F.A. Goudsmit, H.J. Leisi, A.J. Rusi El Hassani, D. Sigg, St. Thomann, W. Volken, D. Bovet, E. Bovet, D. Chatellard, J.-P. Egger, G. Fiorucci, K. Gabathuler, and L.M. Simons, Phys. Lett. B **261**, 16 (1991).
[39] L.M. Simons, in *Muonic Atoms and Molecules*, edited by L.A. Schaller and C. Petitjean (Birkhäuser Verlag, Basel, 1993), p. 307.